

Article

Telomerase inhibitors TMPyP4 and Thymoquinone decreased cell proliferation and induced cell death in NSCLC cell line LC-HK2, modifying the pattern of focal adhesion

A.M. Bernabe Garnique¹, P. Rezende-Teixeira² and G.M. Machado-Santelli¹

¹ Department of Cell and Developmental Biology, Institute of Biomedical Sciences, University of São Paulo, São Paulo, Brazil; anabega@usp.br, glaucia.santelli@gmail.com, gmmsante@usp.br.

² Department of Pharmacology, Institute of Biomedical Sciences, University of São Paulo, São Paulo, Brazil; paularez@gmail.com

* Correspondence: anabega@usp.br, anmibega@gmail.com.

Abstract: G-quadruplexes (G4) are structures formed at the ends of the telomere, these are rich in guanines and were stabilized by molecules that bind to specific sites. TMPyP4 and Thymoquinone (TQ) are small molecules that bind to the G4, they have drawn attention because of their role as telomerase inhibitors. The aim of this study was to evaluate the effects of telomerase inhibitors on cellular proliferation, senescence, and death. Two cell lines LC-HK2 (NSCLC) and RPE-1 were treated with TMPyP4 (5µM) and TQ (10µM). Both inhibitors were effective in decreasing telomerase activity. TMPyP4 increased the percentage of cells with membrane damage associated with cell death and decreased the frequency of cells in the S-phase. TMPyP4 changed the cell adhesion ability and modified the pattern of focal adhesion. TQ acted in a dose-dependent manner, increasing the frequency of senescent cells, and inducing cell cycle arrest in the G1. In conclusion, the effects of both drugs on LC-HK2 and RPE-1 cell lines were different although both are telomerase inhibitors, because TMPyP4 decreased proteins of cell adhesion and TQ induces a decrease in cell viability.

Keywords: TMPyP4 1, Thymoquinone 2, cell viability 3, cell adhesion 4, telomerase.

1. Introduction

G-quadruplexes (G4) are structures formed by four chains of guanine-rich sequences; these structures can be stabilized by monovalent cations forming Hoogsteen bonds [1–3]. *In vivo* evidence has demonstrated the presence of G4 at regulatory regions of genes and at chromosomal ends (telomeres). Different studies have shown control over the expression of oncogenes such as C-MYC, C-KIT, and K-RAS, which can further stimulate recombination in meiosis [2,4–6]. But another important role of G4 is the inhibition of telomerase activity. This is due to the formation of G4 at the tip of telomeres, thus preventing telomerase, the enzyme responsible for the elongation of telomeres, to bind to the telomere and elongate it [1,6]. That characteristic is very important since almost 90% of the described cancers present telomerase activity, whereas only 10% present another type of telomerase elongation independent of telomerase activity. Thus, is for that reason that in recent years different studies have been developed to discover molecules that bind and help to stabilize the G4s.

Monovalent cations like Na⁺ and K⁺ were identified for helping stabilize G4s, and the research for small molecules that bind to G4 increased. Later were developed studies of G4 interaction with different small molecules in cancer cells in culture. [1,2]. Molecules that bind to G4 are capable of leading to telomere dysfunction and chromosomal instability [5–7]. Among these molecules, we highlight the TMPyP4, a molecule derived from a cationic porphyrin that stabilizes G4 and causes telomere dysfunction in addition to other deleterious effects in cancer cells [2,5,8]. Its potential in the inhibition of telomerase activity has been evaluated because it is a G4 stabilizer in the prostate, breast, colon, and other cancer cells [1]. In the study conducted by Lin and colleagues, it was demonstrated that the use of TMPyP4 decreases the growth of ovarian cancer cells, causes modification in

cell morphology, and increases the number of apoptotic bodies, these results were dose-dependent [5].

It was found through cDNA microarray assays that TMPyP4 downregulates the expression of C-MYC oncogene, and this would be responsible for regulating the catalytic subunit of telomerase hTERT activity. Thus, TMPyP4 would be modulated by two different pathways the activity of telomerase [9]. Another study conducted with TMPyP4 combined with photodynamic therapy demonstrated that ovary carcinoma cells suppress cell growth, proliferation, and motility [4].

Another study performed in normal, and cervical carcinoma cells showed that in different concentrations, TMPyP4 would be responsible for the decrease in tumor proliferation and apoptosis of cancer cells by their role in the activation of p38 MAPK pathway signaling. [10].

Similarly, Thymoquinone (TQ) a seed-derived component of *Nigella Sativa* Linn, has been reported as an antitumor agent through different mechanisms and even by associating with telomeric DNA by stabilizing G4 and inhibiting proliferation in cancer cells. [11]. Other *in vivo* studies have shown the anti-tumoral activity of TQ. TQ treatment result in DNA damage, telomere shortening, cell cycle arrest, and apoptosis in cancer and hTERT immortalized cells [12]. Other effects caused by TQ include oxidative damage, inhibition of angiogenesis, migration, invasion, and metastasis of cancer cells [13,14].

A wide variety of responses have been associated with the action of TQ and TMPyP4 in studies in cancer cells *in vivo* and *in vitro*. The elucidation of their effects on cancer cells is of fundamental importance in understanding the action of G4 stabilizer compounds and evaluating their potential as anti-cancer agents. So, the present study aimed to compare the effects of two G4 stabilizing compounds in non-small human lung cancer cells and hTERT immortalized cell line.

2. Materials and Methods

Cell lines

The LC-HK2 cell line from a human non-small cell lung carcinoma, which were established in our laboratory [15], and the commercial line hTERT-RPE-1, Epithelial cells immortalized with hTERT from human retina eye, were grown in Dulbecco's modified Eagle's minimal medium (DMEM) with F-12 (Sigma) nutrient, supplemented with 10% fetal bovine serum (Cultilab). The cultures were kept at 37°C, with the atmosphere containing ~ 5% CO₂. The culture medium was changed every two to three days and the cells were subcultured regularly. Subcultures were obtained by dissociation with 0.05% trypsin solution and 0.02% EDTA.

Inhibitors

Telomerase inhibitors TMPyP4 (CALBIOCHEM) and Thymoquinone (TQ) (SIGMA) were used. The TMPyP4 inhibitor was used at a concentration of 5µM and TQ at concentrations 10µM, this value was obtained from trypan blue cell viability assays. The cell lines were treated for 72 and 144 hours at the above-mentioned concentrations and control samples without inhibitors.

Trypan blue viability assay

Seeded both cell lines and after 24h the cells were treated with the TQ inhibitor at concentrations of 10-100µM. After 24h, the cells were resuspended by trypsin dissociation and added trypan blue to 0.4% 1:1 for 3 minutes. Then, the cells were counted in the Neubauer chamber.

Cell cycle analysis by PI staining

After treatments, cells were resuspended using trypsin-EDTA, centrifuged at 1200 rpm for 10 min, washed with phosphate buffered saline A (PBSA, without Ca⁺ and Mg⁺) and centrifuged. Samples were fixed with 75% methanol at 4°C for 1h and washed with PBSA. The DNA was stained with propidium iodide (10µg/mL) and treated with RNase (10µg/mL) at 4°C for 1 h and quantified by flow cytometer (GUAVA EasyCyte Plus, MA,

USA). The assay was conducted three times in replicates, and the results expressed as mean \pm SD of the percentage of cell distribution in cell cycle phases (G1, S, and G2/M).

Senescence-associated β -galactosidase staining

The senescence assay by β -galactosidase staining was performed by a protocol modified from Stenberg and Timiras and Itahana [16,17]. The cells were fixed with a fresh solution of 3.7% formaldehyde (Sigma-Aldrich) for 20 min at room temperature. Then wash with PBSA and add the staining solution which consists of X-gal (20mg/mL) dissolved in Dimethylformamide; 0.2M citric acid/sodium phosphate solution with pH6; 100mM potassium ferrocyanide; 100 mM potassium ferricyanide; 5M sodium chloride. Seal the plate with parafilm and incubate overnight at 37°C. Coverslips were mounted on microscope slides with 70% glycerol in PBSA.

Immunofluorescence and fluorescence assay

For immunostaining, samples were fixed with 3.7% formaldehyde (Sigma-Aldrich) for 30 min, permeated with Triton X-100 (0.5%) for 30 min and incubated overnight with primary monoclonal antibodies mouse anti- α -Tubulin (1:50, Cell Signaling Technology 3873), mouse anti- β -Tubulin (1:50, Cell Signaling Technology 86298), and 2h with secondary antibodies anti-mouse IgG (H + L), F (ab')₂ Fragment (Alexa Fluor® 555 or 488 Conjugate) (1:50). Nuclei were labeled with DAPI (1:100) or propidium iodide (10mg/mL) from Sigma-Aldrich (MO, USA). The slides were mounted with Vecta-Shield from Vector Laboratories (CA, USA) and analyzed by laser scanning confocal microscopy from Leica TCS SP8 (HE, DE).

Mitotic index

Mitotic index was calculated by manual counting of the number of mitoses/1000 cells per sample from fluorescent cytological preparations stained for microtubules and nuclei. Images were obtained using the Axio Scan Z1 slide scanner microscope (Carl Zeiss Microscopy GmbH, TH, GER) and processing by Zen Blue edition software. The results were expressed as mean \pm SD of the percentage of cells in mitoses/total number of counted cells of three independent experiments.

EdU incorporation

The frequency of S-phase cells was determined by the incorporation of EdU (5-ethynyl-2'-deoxyuridine) using Invitrogen's Click-iT® EdU Imaging kit, following manufacturer's instructions.

Telomerase activity assay

The protocol of Roche's TeloTAG GG Telomerase PCR ELISA plus Kit was used to evaluate telomerase activity. LC-HK2 and RPE-1 cells were plated, and respective treatments were performed with the inhibitors at periods of 72h and 144h.

Cell adhesion assay

Cell adhesion was quantified using the wash adhesion assay. The cells were plated, and after 24h treated with the inhibitor, depending on the treatment period we resuspend the cells with trypsin and placed on a 24-well plate those containing a collagen A background. After approximately 4h incubation, the cells were washed three times with PBSA, and the adherent cells were fixed and stained with violet crystal. After those cells were counted.

Real time PCR assay

The total RNA from control and treated groups of LC-HK2 and RPE-1 cell lines were extracted using the ChargeSwitch Total RNA Cell Kit (Invitrogen) and quantified on a NanoDrop ND1000 Spectrophotometer. Expression profile analysis was performed by real-time RT-PCR reactions on a Corbett Research model Rotor Gene 6000 real-time cyclor and the AgPath-ID One-Step RT-PCR kit (Applied Biosystems). Real-time PCR conditions were 45°C for 10 min; 95°C for 10 min, 40 cycles [95°C for 15 sec; 60°C for 45 sec], following the melt. The primers used were: qVinc1 GCACCCAGCTCAAAATCCTG; qVinc2 TCAGCCAGGTGCCTACTGGT and qVim-left GAGAACTTTGCCGTTGAAGC; qVim-right TCCAGCAGCTTCCTGTAGGT, which amplify fragments of up to 250 bases and normalization was done by the total mass of RNA used by reaction, as suggested by Bustin (2000, 2002).

Zombie green assay

Cells with membrane damage, which may have been caused by inhibitor treatments, were evaluated by the Zombie Green assay using the Zombie Green™ Fixable Viability Kit (Biolegend).

Statistical analysis

Results were expressed as mean (SD). Data were submitted to the ANOVA test, followed by Dunnett's test for multiple comparisons with the control. p-value <0.05 was considered statistically significant.

3. Results

Cell viability assay for Thymoquinone

TQ showed antitumor potential by inhibiting cell proliferation and inducing apoptosis [18], as well as by the formation of G4. Thus, the cell viability assay was performed for trypan blue staining, cells were treated with TQ at concentrations of 10 – 100µM and a dose-dependent reduction in cell viability was observed in both cell lines (RPE-1 and LC-HK2). LC-HK2 cell line showed a decrease in cell viability compared to control, in 20, 40, 80, and 100µM were 79.56%, 61.65%, 25.31%, and 9.87% of viable cells, respectively (Figure 1).

In the RPE-1 cell line, this reduction was more accentuated in the highest concentrations, the cell viability in the control was 98%, and the treated cells with 20, 40, 80, and 100µM were 73%, 65.66%, 8.73%, and 3.63%, respectively (Figure 1).

So, to analyse the induction of cellular senescence, the TQ concentration used in cell treatments was 10µM a non-lethal concentration and the treatments were performed for 72 and 144h (Figure 1).

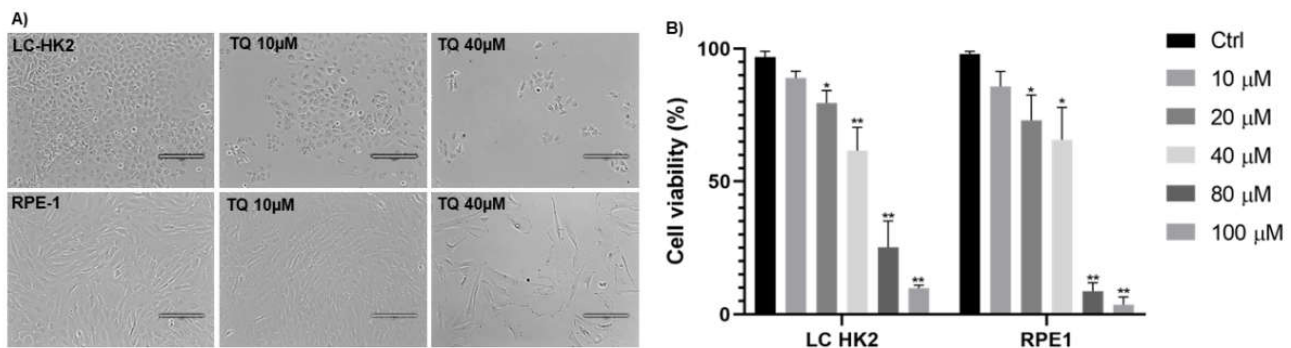


Figure 1 - Cell viability assay of TQ treated LC-HK2 and RPE-1 cell lines: A) Phase contrast image of LC-HK2 and RPE-1 cell lines in control and TQ treatment (10 and 40µM) conditions. Bar scale: 200 µm. B) Both cell lines were treated with TQ at concentrations of 10-100µM for 24h. Data are shown as percentages of average relative to control in three independent experiments. Statistical analysis was performed by Dunnett - ANOVA test for multiple comparisons *vs* control. ** <0.01 and * P value <0.05.

TMPyP4 and Thymoquinone inhibit telomerase activity triggering senescence, cell death and membrane damage

The effect of TMPyP4 and TQ on telomerase activity was evaluated. The treatment with TMPyP4 (5µM) for 72h reduced the telomerase activity in LC-HK2 and RPE-1 cells to 0.74 and 0.81, respectively, compared to control cells (Figure 2A). Cells treated with TQ (10µM) showed also decreased telomerase activity, in LC-HK2 cells was 0.88 and 0.87 in RPE-1 cells (Figure 2A). Circular dichroism is one of the methods used to show that TMPyP4 and TQ interact with the telomere forming G4, inhibiting the binding of the telomerase enzyme, this decrease can be caused for this action in the telomere. [11,19].

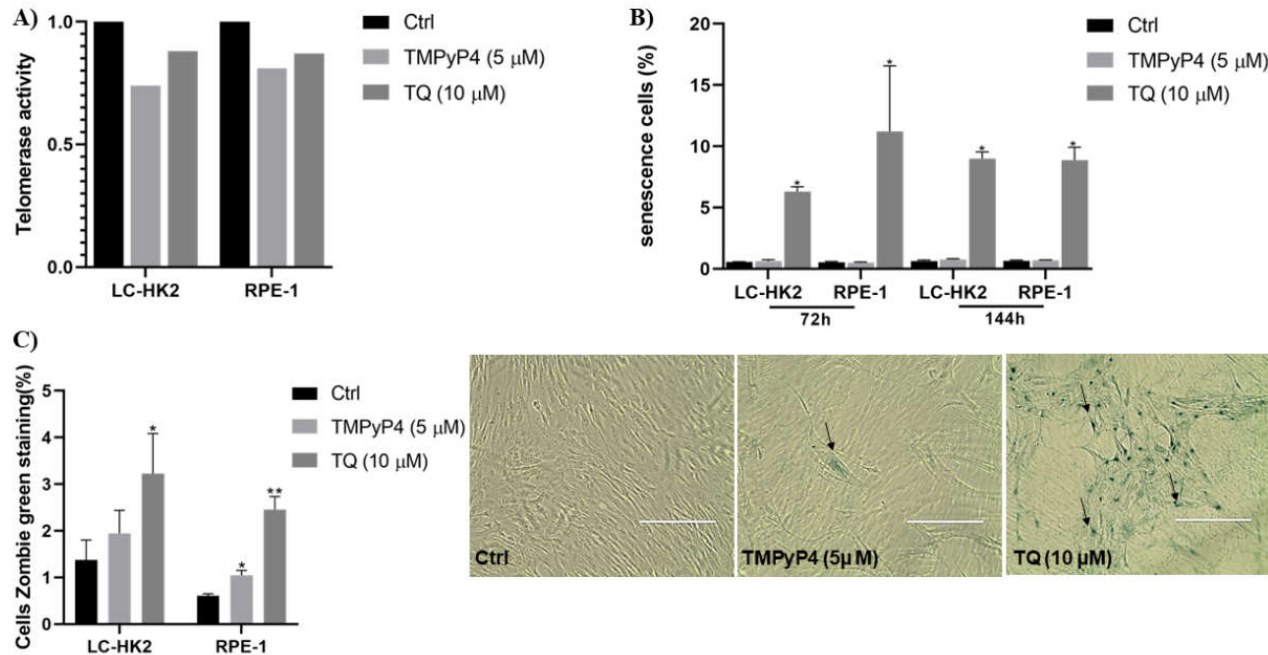


Figure 2 - Telomerase activity, senescence, cell death and membrane damage. A) Evaluation of telomerase activity in LC-HK2 and RPE-1 cells treated with TMPyP4 (5 μ M) and TQ (10 μ M) inhibitors for 72 h to evaluate telomerase activity. Data are shown as averages of two independent experiments. B) Percentage of senescent cells treated with telomerase inhibitors. Increase in senescent cells treated with TQ (10 μ M) after 72 and 144h. Data are shown as percentages of averages relative to control in three independent experiments. Statistical analysis was performed by Dunnett - ANOVA test for multiple comparisons *vs* control. ** <0.01 and * P value <0.05. In the low panel is being shown senescence assay on RPE-1 cells treatment with TMPyP4 (5 μ M) and TQ (10 μ M). C) Percentage of cells with membrane damage treated with telomerase inhibitors. Data are shown as percentages of averages relative to control in three independent experiments. Statistical analysis was performed by Dunnett - ANOVA test for multiple comparisons *vs* control. * P value <0.01.

One of the characteristics of senescent cells is the induction of expression of senescence-associated β -Galactosidase (SA- β -Gal), in addition to flat morphology [20]. LC-HK2 and RPE-1 cell lines treated with TMPyP4 (5 μ M) for 72h showed a frequency of senescent cells of 0.63% and 0.5%, respectively. The control cells showed 0.57% in LC-HK2, and 0.54% in RPE-1, in the same treatment period (Figure 2B). After 144 h, the control cells showed 0.64% in LC-HK2 and 0.65% in RPE-1, and the treatment with TMPyP4 (5 μ M) had a senescent cell percentage of 0.77% and 0.7% in LC-HK2 and RPE-1, respectively (Figure 2B).

TQ (10 μ M) showed an increase in the percentage of senescent cells, in the LC-HK2 cells, the percentage of senescent cells was 6.3% (72h), and 8.9% (144h). And RPE-1 cells showed a high pronounced response of senescent cells of 11.23% (72h) and 8.87 (144h) (Figure 2B).

As a reduction in the percentage of cells was observed in the treatments with TQ to evaluate cell death the Zombie Green assay was performed, which marks the cells that suffered damage to the cell membrane.

The LC-HK2 cell line treated with TMPyP4 had membrane damage on 1.94% of its cells compared to 1.37% in control cells and when treated with TQ (10 μ M) this percentage was 3.22% at 72h (Figure 2C). In RPE-1 cells had 0.61% of cells labeled with cell membrane damage in the control, and cells treated with TMPyP4 (5 μ M) had 1.04%. Whereas the treatment with TQ (10 μ M) showed 2.45% of cells with membrane damage after 72h, indicating an increase in cells with membrane damage that will be forwarded for death caused by treatments with the inhibitors (Figure 2C).

TMPyP4 and Thymoquinone Telomerase Inhibitors modify cell proliferation

The cell proliferation was evaluated by flow cytometry assay, EdU incorporation, and mitotic index. For cell cycle profile evaluation, cells were treated with both inhibitors and staining with PI for cytometry. Cells treated with TMPyP4 (5µM) showed differences in cell cycle phases (Figure 3), after 72h of treatment it was observed an increase in the G0/G1 phase cell population compared to control cells, the frequency observed was 56.9% for LC-HK2 and 67.65% for RPE-1. And the cell population in the S phase was 16.66% for LC-HK2 and 8.3% for RPE-1, which showed a decrease compared to control cells. After 144h of treatment in the LC-HK2 cells was observed increase in cell population in the G0/G1 phase (51.62%) with a decrease in S (19.43%) and G2/M (23.24%) phase cells. RPE-1 cells showed a decrease in the S phase cell population (8.23%) (Figure 3).

TQ (10µM) treatments (72h) of LC-HK2 cells a decrease in the S phase cell population (20.51%) was observed. In RPE-1 cells treated with TQ (10µM), there was a decrease in the S phase (5%) and an increase in sub-G1 (2.27%), G1 (65.67%), and G2/M (26.27%) phases. In analyzes of the treatments with TQ (10µM) for 144h, LC-HK2 cells showed an increase in the G1 phase (54.52%) and a decrease in S (15.55%) and G2/M (22.94%) phases. The RPE-1 cells showed an increase in sub-G1 (2.49%) and G0/G1 (65.78%) phases, with a decrease in S (7.51%) phase (Figure 3).

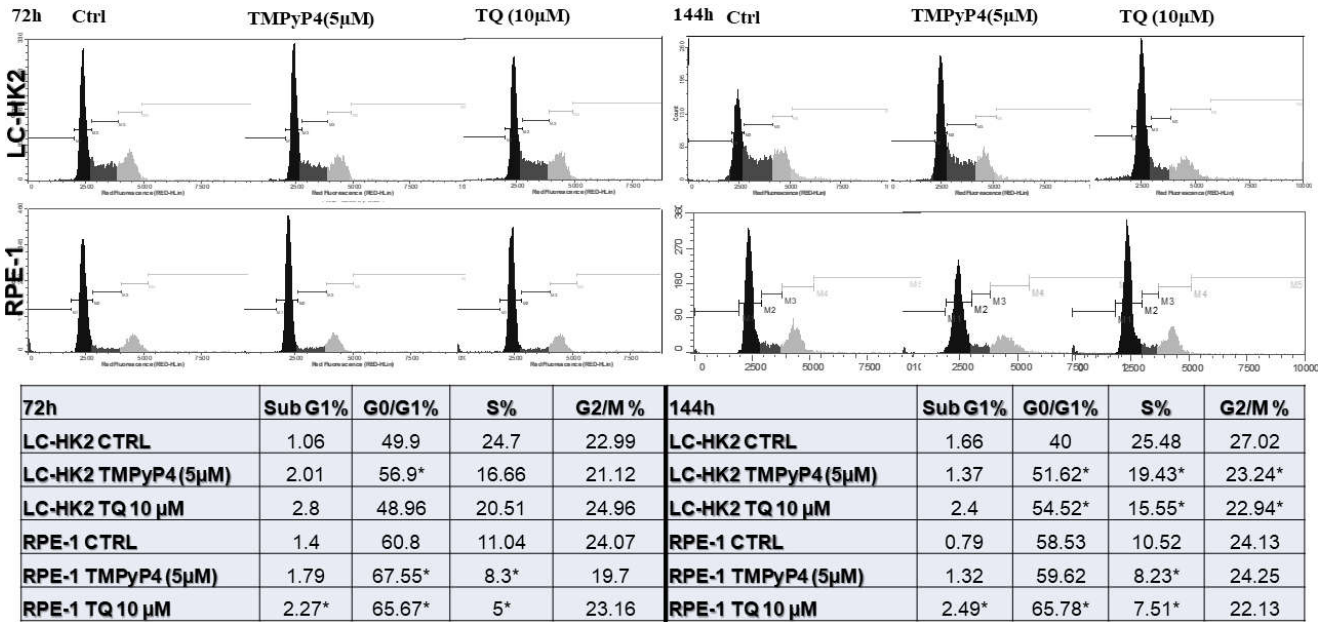


Figure 3 - Distribution of cell cycle phases: LC-HK2 and RPE-1 treated with TMPyP4 (5µM) and TQ (10µM) for 72h and 144h showed increase in some phases of the cell cycle, as well as difference in response to treatments depending on the cell line. Data are shown as percentages of averages relative to control in three independent experiments. Statistical analysis was performed by Dunnett - ANOVA test for multiple comparisons vs control. * P value <0.05.

Mitotic index and EdU assay

The mitotic index was analyzed by counting the number of cells in mitosis. The treatment with TQ (10µM) in the LC-HK2 cell line after 72h showed 2.24% of mitotic cells, and the control cells showed 5.23%. In the RPE-1 cell line, after the same period, the treatment with TQ (10µM) decreased the percentage of mitotic cells to 2.51%, compared to 4.83% in control cells (Figure 4A).

After 144h, the treatment with TMPyP4 (5µM) was observed that the LC-HK2 cell line increase the number of mitotic cells, that was 4.1% and the control cells were 3.44%. And when treated with TQ (10µM), we observed a decrease of mitotic cells that was 2.62%. The RPE-1 cell line just was observed to decrease in mitotic cells, after the treatment with

TQ (10 μ M) we counted 1.26% of mitotic cells, and the control cells were 2.53% (Figure 4A).

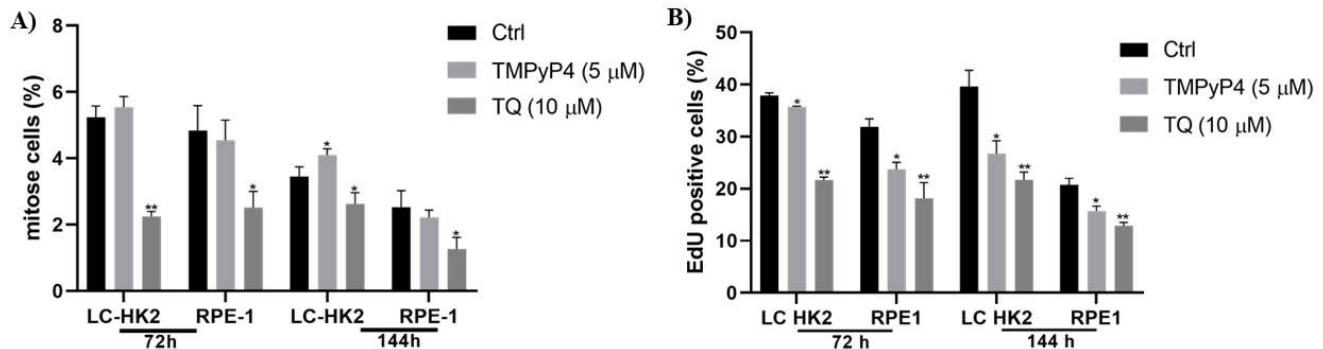


Figure 4: A) Percentage of mitotic cells: Decrease of mitotic cells was observed when treated with the inhibitors. Statistical analysis was performed by Dunnett - ANOVA test for multiple comparisons *vs* control. ** <0.01 and * P value <0.05. B) Percentage of EdU-labeled cells: A decrease in EdU-positive cells was observed when treated with the inhibitors. Data are shown as percentages of averages relative to control in three independent experiments. Statistical analysis was performed by Dunnett - ANOVA test for multiple comparisons *vs* control. ** and * P value <0.05.

The EdU assay was performed to determine the number of cells in the S phase of the cell cycle. After treatment with the inhibitors, a decrease in the number of cells in the synthesis phase was observed. The LC-HK2 and RPE-1 cell lines showed in control 37.86% and 31.86%, respectively, of cells in the S phase. After the treatment with TMPyP4 (5 μ M) for 72h, the LC-HK2 cell line was 35.66% and 23.74% in the RPE-1 cell line. And the treatment with TQ (10 μ M) was found at 21.63% and 18.15% in LC-HK2 and RPE-1 cell lines, respectively (Figure 4B).

In the time of 144h, the reduction in the percentage of cells in the S phase was sustained. LC-HK2 and RPE-1 control cells showed 39.61% and 20.72%, respectively. The treatment with TMPyP4 (5 μ M) showed 26.73% in LC-HK2 and 15.68% in RPE-1 cells, and finally, the treatment with TQ (10 μ M) was observed at 21.67% for LC-HK2 and 12.9% for RPE-1 cells (Figure 4B).

TMPPyP4 causes alteration in actin cytoskeleton and cell adhesion

The cells treated with TMPPyP4 inhibitor became more difficult to detach from the cell culture plate when was used the trypsin-EDTA solution, requiring at least twice as long as the control or the TQ-treated cells to detach. For this reason, the cell adhesion assay and immuno-fluorescence of focal adhesion protein and cytoskeleton of actin labeling were performed.

For the cellular adhesion assay, the cells after the treatment with the inhibitors were seeded in plates containing collagen at the bottom to adhere and after 4 hours, the cells were washed and stained, then the number of cells that remained adhered was counted. Treatments with TMPPyP4 (5 μ M) lead to a decrease in surface-adhered LC-HK2 cells. After 72h was observed 70.78% and after 144h was observed 83.26% of cells adhered. For RPE-1 cells the treatment TMPPyP4 (5 μ M) lead 91.8% after 72h and after 144h was observed that 77.3% of cells remained adhered. In cells treated with TQ (10 μ M), there was a decrease in the number of adherent cells, after 72h LC-HK2 had 29.53% and RPE-1 62.32% of cells. After 144h was observed 33.35% in LC-HK2 and 42.7% in RPE-1 cells (Figure 5A).

Immunofluorescence of vinculin protein evidenced focal adhesion structures in RPE-1 in control and treated cells with TQ (10 μ M). But when analyzing cells treated with TMPPyP4 (5 μ M), the focal adhesion structures do not form (Figure 5B). In the same way, the cytoskeleton of actin was staining and was observed that this structure follows the

focal adhesion in the control cells, but this was not observed in the treated cells with TMPyP4 (5 μ M) (Figure 5B, the cytoskeleton of actin is in blue).

Then, the expression of vinculin and vimentin mRNA in the cells treated with the TMPyP4 (5 μ M) were analyzed, both have an association with the superficial-cell binding process. Downregulation of these mRNAs was already observed in both cell lines after 72h, and the downregulation persisted until 144h (Figure 5C).

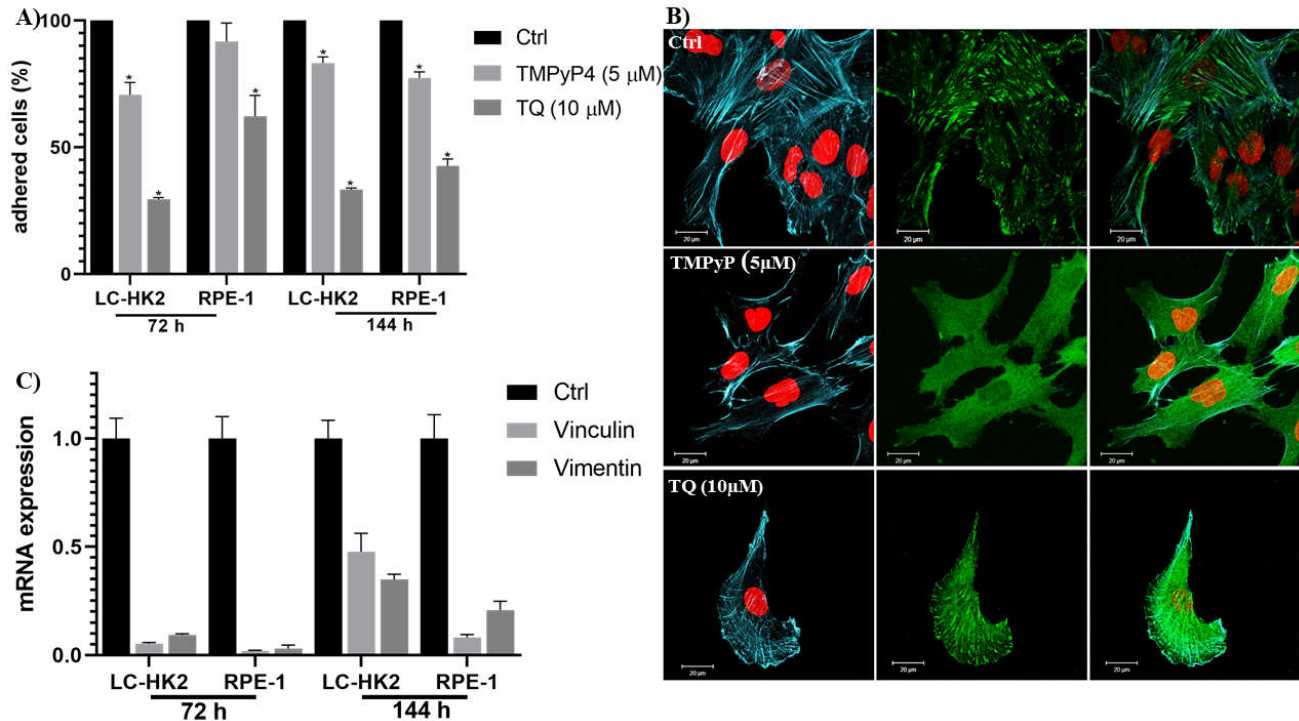


Figure 5 - A) Percentage of adherent cells after treatment with inhibitors: Statistical analysis was performed by Dunnett - ANOVA test for multiple comparisons *vs* control. * P value <0.01 **B)** Immunofluorescence of focal adhesions formed by vinculin protein: Cells treated for 72h with the TMPyP4 inhibitor did not show the focal adhesion (green) formed by vinculin, whereas in control and treated cells with TQ (10 μ M) it can be seen. Nucleus in red and in blue actin cytoskeleton. Bar Scale 20 μ m. **C)** Expression of vinculin and vimentin mRNA in TMPyP4 treated cells: A decrease in vinculin and vimentin expression is observed after 72 h and 144h.

Discussion

Thymoquinone and TMPyP4 decrease of telomerase activity

It is known that TMPyP4 is an inhibitor of telomerase, and TQ can behave similar [11]. Telomerase activity can be inhibited through G4 stabilization. The telomerase activity assay showed that TQ and TMPyP4 can cause a decrease in telomerase activity in both tested cell lines (LC-HK2 and RPE-1), considering that the RPE-1 cell line is immortalized by activating telomerase expression.

TQ decrease cell viability, induce senescence and arrest in the cell cycle

It was observed that TQ reduced cellular viability after treatment with increased concentrations of TQ (10 – 100 μ M), and this effect was increased with the exposition time in both cell lines. In the same way, we observed an increase in the cell number with membrane damage which can be forward to cell death, this kind of death was registered in other studies as apoptosis with to Bax and Bcl2 signalization [21,22].

It is worth mentioning that Berehab and colleagues studies with TQ did not demonstrate an effect on the viability of no tumoral cells [23], but in the present study, TQ was able to decrease the cell viability of the RPE-1 cell, a no tumoral cell line immortalized

with hTERT which result in telomerase activation. Thus, this cell viability decreased could be an answer to the association between TQ binding with G4.

Stochastic telomere attrition or genotoxic stress can cause dysfunctional telomere, induced cellular senescence, in this way helping in the inhibition of tumour progression [24,25]. The study on glioblastoma cells demonstrated that TQ can be responsible to cause this dysfunction [12]. We showed that TQ increased the number of senescent cells in LC-HK2 and RPE-1, but this was dependent on the time and concentration which were the treated cells.

We observed arrest in the G1 phase and decrease in the S phase caused by TQ treatment, this effect was similar in both cell lines. This effect was also described in hepatocellular carcinoma, where TQ caused arrest in the G1 phase with a consequent decrease in the number of cells in the S phase. Therefore, it was observed that TQ action depends on the concentration and the time in which cells were exposed because it can be caused senescence or death by signalization of pro-apoptotic proteins [22].

TMPyP4 exert influence on cellular adhesion

He and colleagues demonstrated that the formation of G4 can affect the binding of the transcription factor to the nearby binding site, which may cause additional influence on gene transcription [26]. G-quadruplex intrachain and G-quadruplex forming sequences may coincide with promoter regions and play a role in transcriptional regulation or be found at replication origin sites. In addition, it was observed that G4 forms preferentially in regions rich in guanine [27].

The TMPyP4 inhibitor used at a concentration of 5uM led to a decrease in telomerase activity and changes in the cell cycle, without causing high damage to cell viability at the analyzed times. However, changes in cell adhesion to the substrate were observed as demonstrated by the cell adhesion assay.

Zheng and colleagues demonstrated through of RNA-seq analysis of the whole genome of the A549 cell line, that TMPyP4 can alter gene expression. These changes can be positively or negatively depending on the concentration of this compost and the genes found are associated with adhesion, migration, and cell death [28]. So, we analyzed proteins associated with cell adhesion and motility, such as vinculin and vimentin, and as demonstrated in immunofluorescence and mRNA expression assays this expression is changed in treated cells with TMPyP4.

Vinculin is a protein that participates in the formation of focal adhesions, having a role in the motility and organization of the actin cytoskeleton, exerting a direct influence on cell migration. Downregulation of vinculin levels has been associated with reduced adhesion and improved cell motility [29].

Decreased expression of vinculin mRNA levels accompanied by a decrease in vimentin mRNA was observed. Peng and colleagues, performed vimentin silencing and observed that vimentin along with actin cytoskeleton remodeling is required for docking and detachment after cell migration and that this interaction leads to improved tumor cell invasion[30]. In this work, a decrease in the levels of vinculin and vimentin was observed, which could be helping in the detachment of the cells, later the levels of vimentin begin to be reestablished, and together with the formation of stress fibers and the migration control can be resumed, this was the effect observed in the first days of treatments with TMPyP4.

5. Conclusions

The TMPyP4 and TQ are considered inhibitors of telomerase because are capable of binding at telomere to prevent telomerase activity. This study demonstrated that these compounds decreased the telomerase activity but too were able to generate different responses in the proliferation, viability, and senescence cell, so as in proteins associated with cell adhesion, and this effect depends on the concentration and time of treatment that cells are subject.

Author Contributions: All authors have read and agreed to the published version of the manuscript”.

Funding: “This research was funded by COORDENAÇÃO DE APERFEIÇOAMENTO DE NÍVEL SUPERIOR (CAPES), FUNDAÇÃO DE AMPARO A PESQUISA DO ESTADO DE SÃO PAULO (FAPESP) grant: 2015/17177–6, Conselho Nacional de Desenvolvimento Científico e tecnológico (CNPq) grant 303464/2017-8

Data Availability Statement: Not applicable.

Acknowledgments: Not applicable.

Conflicts of Interest: The authors declare no conflict of interest.

References

1. Rhodes, D.; Lipps, H.J. Survey and Summary G-Quadruplexes and Their Regulatory Roles in Biology. *Nucleic Acids Res.* **2015**, *43*, 8627–8637.
2. Murat, P.; Singh, Y.; Defrancq, E. Methods for Investigating G-Quadruplex DNA/Ligand Interactions. *Chem. Soc. Rev.* **2011**, *40*, 5293–5307, doi:10.1039/c1cs15117g.
3. Rizzo, A.; Salvati, E.; Biroccio, A. Methods of Studying Telomere Damage Induced by Quadruplex-Ligand Complexes. *Methods* **2012**, *57*, 93–99, doi:10.1016/j.ymeth.2012.02.010.
4. Liu, H.; Lv, C.; Ding, B.; Wang, J.; Li, S.; Zhang, Y. Antitumor Activity of G-Quadruplex-Interactive Agent TMPyP4 with Photodynamic Therapy in Ovarian Carcinoma Cells. *Oncol. Lett.* **2014**, *8*, 409–413, doi:10.3892/ol.2014.2125.
5. Lin, W.; Sampathi, S.; Dai, H.; Liu, C.; Zhou, M.; Hu, J.; Huang, Q.; Campbell, J.; Shin-Ya, K.; Zheng, L.; et al. Mammalian DNA2 Helicase/Nuclease Cleaves G-Quadruplex DNA and Is Required for Telomere Integrity. *EMBO J.* **2013**, *32*, 1425–1439, doi:10.1038/emboj.2013.88.
6. Biffi, G.; Tannahill, D.; McCafferty, J.; Balasubramanian, S. Quantitative Visualization of DNA G-Quadruplex Structures in Human Cells. *Nat. Chem.* **2013**, *5*, 182–186, doi:10.1038/nchem.1548.
7. Zhou, G.; Liu, X.; Li, Y.; Xu, S.; Ma, C.; Wu, X.; Cheng, Y.; Yu, Z.; Zhao, G.; Chen, Y. *Telomere Targeting with a Novel G-Quadruplex-Interactive Ligand BRACO-19 Induces T-Loop Disassembly and Telomerase Displacement in Human Glioblastoma Cells*; 2016; Vol. 7;.
8. Müller, S.; Rodriguez, R. G-Quadruplex Interacting Small Molecules and Drugs: From Bench toward Bedside. *Expert Rev. Clin. Pharmacol.* **2014**, *7*, 663–679.
9. Grand, C.L.; Han, H.; Muñ Oz, M.; Weitman, S.; Hoff, D.D. Von; Hurley, L.H.; Bearss, D.J. *The Cationic Porphyrin TMPyP4 Down-Regulates c-MYC and Human Telomerase Reverse Transcriptase Expression and Inhibits Tumor Growth in Vivo* **1**; 2002;
10. Cheng, M.J.; Cao, Y.G. TMPYP4 Exerted Antitumor Effects in Human Cervical Cancer Cells through Activation of P38 Mitogen-Activated Protein Kinase. *Biol. Res.* **2017**, *50*, doi:10.1186/s40659-017-0129-4.
11. Salem, A.A.; El Haty, I.A.; Abdou, I.M.; Mu, Y. Interaction of Human Telomeric G-Quadruplex DNA with Thymoquinone: A Possible Mechanism for Thymoquinone Anticancer Effect. *Biochim. Biophys. Acta - Gen. Subj.* **2015**, *1850*, 329–342, doi:10.1016/j.bbagen.2014.10.018.
12. Gurung, R.L.; Lim, S.N.; Khaw, A.K.; Soon, J.F.F.; Shenoy, K.; Ali, S.M.; Jayapal, M.; Sethu, S.; Baskar, R.; Prakash Hande, M. Thymoquinone Induces Telomere Shortening, DNA Damage and Apoptosis in Human Glioblastoma Cells. *PLoS One* **2010**, *5*, doi:10.1371/journal.pone.0012124.
13. Khan, M.A.; Tania, M.; Fu, S.; Fu, J. *Thymoquinone, as an Anticancer Molecule: From Basic Research to Clinical Investigation*; 2017; Vol. 8;.
14. Kundu, J.; Chun, K.S.; Aruoma, O.I.; Kundu, J.K. Mechanistic Perspectives on Cancer Chemoprevention/Chemotherapeutic

- Effects of Thymoquinone. *Mutat. Res. - Fundam. Mol. Mech. Mutagen.* 2014, 768, 22–34.
15. Bonaldo MF; Pestano MC; Ribeiro MC; Machado-Santelli GM; Mori Loa *Comparative Characterization Of A Human Large Cell Lung Carcinoma Cell Line And The Xenograft Derived Cell Line*;
 16. Sternberg Hal; Timiras Paola. *Studies of Aging*; 1999;
 17. Itahana, K.; Campisi, J.; Dimri, G.P. *Methods to Detect Biomarkers of Cellular Senescence The Senescence-Associated-Galactosidase Assay*; 2007;
 18. Attoub, S.; Sperandio, O.; Raza, H.; Arafat, K.; Al-Salam, S.; Al Sultan, M.A.; Al Safi, M.; Takahashi, T.; Adem, A. Thymoquinone as an Anticancer Agent: Evidence from Inhibition of Cancer Cells Viability and Invasion in Vitro and Tumor Growth in Vivo. *Fundam. Clin. Pharmacol.* **2013**, 27, 557–569, doi:10.1111/j.1472-8206.2012.01056.x.
 19. Dupont, J.I.; Henderson, K.L.; Metz, A.; Le, V.H.; Emerson, J.P.; Lewis, E.A. Calorimetric and Spectroscopic Investigations of the Binding of Metallated Porphyrins to G-Quadruplex DNA. *Biochim. Biophys. Acta - Gen. Subj.* **2016**, 1860, 902–909, doi:10.1016/j.bbagen.2015.09.004.
 20. Sharpless, N.E.; DePinho, R.A. Telomeres, Stem Cells, Senescence, and Cancer. *J. Clin. Invest.* **2004**, 113, 160–168, doi:10.1172/jci200420761.
 21. Liu, X.; Dong, J.; Cai, W.; Pan, Y.; Li, R.; Li, B. The Effect of Thymoquinone on Apoptosis of SK-OV-3 Ovarian Cancer Cell by Regulation of Bcl-2 and Bax. *Int. J. Gynecol. Cancer* **2017**, 27, 1596–1601, doi:10.1097/IGC.0000000000001064.
 22. Ke, X.; Zhao, Y.; Lu, X.; Wang, Z.; Liu, Y.; Ren, M.; Lu, G.; Zhang, D.; Sun, Z.; Xu, Z.; et al. *TQ Inhibits Hepatocellular Carcinoma Growth in Vitro and in Vivo via Repression of Notch Signaling*; Vol. 6;.
 23. Berehab, M.; Rouas, R.; Akl, H.; Duvillier, H.; Journe, F.; Fayyad-Kazan, H.; Ghanem, G.; Bron, D.; Lewalle, P.; Merimi, M. Apoptotic and Non-Apoptotic Modalities of Thymoquinone-Induced Lymphoma Cell Death: Highlight of the Role of Cytosolic Calcium and Necroptosis. *Cancers (Basel)*. **2021**, 13, doi:10.3390/cancers13143579.
 24. Suram, A.; Herbig, U. The Replicometer Is Broken: Telomeres Activate Cellular Senescence in Response to Genotoxic Stresses. *Aging Cell* 2014, 13, 780–786.
 25. Subburayan, K.; Thayyullathil, F.; Pallichankandy, S.; Rahman, A.; Galadari, S. Par-4-Dependent P53 up-Regulation Plays a Critical Role in Thymoquinone-Induced Cellular Senescence in Human Malignant Glioma Cells. *Cancer Lett.* **2018**, 426, 80–97, doi:10.1016/j.canlet.2018.04.009.
 26. He, Q.; Zeng, P.; Tan, J.H.; Ou, T.M.; Gu, L.Q.; Huang, Z.S.; Li, D. G-Quadruplex-Mediated Regulation of Telomere Binding Protein POT1 Gene Expression. *Biochim. Biophys. Acta - Gen. Subj.* **2014**, 1840, 2222–2233, doi:10.1016/j.bbagen.2014.03.001.
 27. Raiber, E.A.; Kranaster, R.; Lam, E.; Nikan, M.; Balasubramanian, S. A Non-Canonical DNA Structure Is a Binding Motif for the Transcription Factor SP1 in Vitro. *Nucleic Acids Res.* **2012**, 40, 1499–1508, doi:10.1093/nar/gkr882.
 28. Zheng, X.H.; Nie, X.; Liu, H.Y.; Fang, Y.M.; Zhao, Y.; Xia, L.X. TMPyP4 Promotes Cancer Cell Migration at Low Doses, but Induces Cell Death at High Doses. *Sci. Rep.* **2016**, 6, doi:10.1038/srep26592.
 29. Toma-Jonik, A.; Widlak, W.; Korfanty, J.; Cichon, T.; Smolarczyk, R.; Gogler-Piglowska, A.; Widlak, P.; Vydra, N. Active Heat Shock Transcription Factor 1 Supports Migration of the Melanoma Cells via Vinculin Down-Regulation. *Cell. Signal.* **2015**, 27, 394–401, doi:10.1016/j.cellsig.2014.11.029.
 30. Peng, J.M.; Chen, W.Y.; Cheng, J.H.; Luo, J.W.; Tzeng, H.T. Dysregulation of Cytoskeleton Remodeling Drives Invasive Leading Cells Detachment. *Cancers (Basel)*. **2021**, 13, doi:10.3390/cancers13225648.